

# PHYSICAL REVIEW B

## CONDENSED MATTER

THIRD SERIES, VOLUME 45, NUMBER 11

15 MARCH 1992-I

### Total energy and band structure of the 3*d*, 4*d*, and 5*d* metals

M. Sigalas

*Research Center of Crete, P.O. Box 527, GR-711 10 Heraklion, Greece*

D. A. Papaconstantopoulos

*Complex Systems Theory Branch, Naval Research Laboratory, Washington, D.C. 20375-5000*

N. C. Bacalis

*National Hellenic Research Foundation, GR-11635 Athens, Greece*

(Received 18 October 1991)

We performed total-energy calculations by the scalar-relativistic augmented-plane-wave method in the local-density and muffin-tin approximations for all 3*d*, 4*d*, and 5*d* transition metals in the fcc and bcc structures. These calculations predict the correct equilibrium structure and give good agreement with experiment and other calculations for lattice constants and bulk moduli.

#### I. INTRODUCTION

The relative stability of crystal structures in the transition metals has been explained by Pettifor<sup>1</sup> using a model characterized by only two *d*-resonance parameters, from which the densities of states were obtained in a hybrid nearly-free-electron and tight-binding scheme. The simple approach of Pettifor worked surprisingly well considering that it was based on differences of the total one-electron band-structure energies neglecting contributions to the total energy from the electrostatic double counting and the exchange and correlation terms. Subsequently, Andersen and co-workers<sup>2,3</sup> and Heine<sup>4</sup> demonstrated the cancellation of the double counting and exchange-correlation terms provided that the electron potential is frozen from one structure to the other. This approach, referred to as Andersen's force theorem, was taken by Skriver,<sup>5</sup> who used the linear muffin-tin orbital (LMTO) method to calculate the relative stability of all elements. Skriver went beyond the essentially canonical approximation employed by Pettifor including hybridization with *sp* bands. Skriver performed a self-consistent (SC) calculation for each element in the fcc structure, and then used the SC fcc potential to calculate the sum of one-electron energies for the bcc structure. The resulting difference of the band structure energies gave him the correct ordering of total energies between different structures for all elements except Au.

In the present paper we present systematic calculations of the total energy of all the 3*d*, 4*d*, and 5*d* transition metals as well as the alkaline earth elements. Our calcu-

lations were performed by the semirelativistic augmented-plane-wave (APW) method in the muffin-tin approximation; they were done fully self-consistently for both the fcc and bcc structures without using the frozen potential procedure employed by Skriver. In this sense our calculations are similar to those of Davenport, Watson, and Weinert,<sup>6</sup> who studied the 5*d* series by the linear augmented Slater-type-orbital method. Our results for the lattice parameters and bulk moduli agree with those of Moruzzi, Janak, and Williams<sup>7</sup> with small differences due to neglect of relativistic effects in the latter calculations.

This article is organized as follows. Section II describes the method of calculation and the approximations. Section III contains our results in comparison with values from the experiment and previous calculations. In Sec. IV we discuss trends in the band structure, and in Sec. V we summarize the results.

#### II. METHOD OF CALCULATION AND APPROXIMATIONS

The total energy was calculated from the expression of Janak,<sup>8</sup> which is valid within the muffin-tin (MT) approximation and needs the crystal potential, the charge density, and the eigenvalue sum as input. These were calculated self-consistently with the symmetrized APW method<sup>9</sup> using the MT approximation, which is accurate<sup>10</sup> for cubic materials. The crystal potential was calculated on a doubling linear mesh consisting of 730 points inside the MT radius. We have found that an integration with a

smaller number of points leads to errors in the total energy of 1–8 mRy depending on the atomic number. For example, for Ca the errors are about 1 mRy, but for Cd they are about 8 mRy. The logarithmic derivatives were calculated on a mesh of at least 500 points per Ry to ensure good eigenvalue convergence.

To determine the charge density and the potential self-consistently we treated the highest  $p$ ,  $s$ , and  $d$  orbitals as band levels, but the stability of the structure was unchanged if we used only  $s$  and  $d$  orbitals as bands. All other states were treated as core levels because they form essentially flat bands. The core levels were calculated by a fully relativistic atomiclike calculation in each iteration. The band states were calculated self-consistently in the semi-relativistic approximation<sup>12</sup> (the spin-orbit coupling is neglected) initially on an equally spaced mesh of  $20k$  points in the irreducible zone for the fcc, and  $14k$  points for the bcc structure. However, to achieve satisfactory convergence it was necessary to use  $89-k$  point sampling for the fcc and  $55k$ -point for the bcc structures. The errors in the total energy which could arise by using smaller  $k$ -point sampling were 1–8 mRy for bcc and 0.2–3 mRy for the fcc structure.

A convergence in the energy levels of 0.5 mRy assured a convergence in the total energy of less than 0.05 mRy. In all our calculations the exchange potential was treated in the exchange and correlation formalism of Hedin and Lundqvist,<sup>13</sup> which is accurate for ground-state properties. To find the equilibrium lattice constants we calculated the total energy at various lattice constants, and determined the minimum by fitting the results with a parabolic or cubic least-squares fit, with rms errors less than 0.2 mRy, as proposed by Birch.<sup>14</sup>

### III. COMPARISON WITH EXPERIMENT AND OTHER CALCULATIONS

Comparing our results with experiment<sup>15</sup> we find a nearly perfect agreement especially for the  $4d$  metals where magnetic behavior is absent.<sup>16,17</sup> As is usually the case in the local-density approximation (LDA), our predicted lattice constants are slightly less than the experimental values and the bulk moduli are overestimated. For the  $3d$  and  $4d$  elements where we can make direct comparison with experiment we find that the calculated lattice constants are 2–5 % smaller and that the bulk moduli are 10–15 % larger than experiment. For the  $5d$  elements our calculated values are in much better agreement with experiment. The percentage errors are within 1% and 6% for the equilibrium volume and bulk modulus, respectively. For the alkaline-earth metals we find the largest discrepancies with experiment similar to the findings of other calculations.<sup>7</sup> This is probably due to the fact that these metals undergo a semimetallic phase transition under pressure,<sup>18</sup> which makes non-muffin-tin corrections become important. Such corrections may also improve the results for the more open bcc structure.<sup>11</sup>

Our results are presented in Tables I–III. We note from these tables that along each  $d$  row of the periodic table the unit cell volume (or the lattice constant) decreases with the atomic number  $Z$  until the eighth column (Fe, Ru, Os) and then increases toward the end of the row. Conversely, the bulk modulus  $B_0$  reaches a maximum at the eighth column where the lattice constant is at a minimum. These results of the variation in  $a_0$  and  $B_0$  with  $Z$  reflect the fact that the filling of the  $d$

TABLE I. Bulk moduli ( $B_0$ ), equilibrium total energy ( $E_{\text{tot}}$ ), volume per atom ( $V_0$ ), and the total energy difference ( $\Delta E$ ) between bcc and fcc for  $3d$  metals.

System	$E_{\text{tot}}$ (Ry)	$\Delta E$ (mRy)	$V_0$ (a.u. <sup>3</sup> )		$B_0$ (Mbar)	
			theor.	expt.	theor.	expt.
fcc Ca	–1357.5271		248.36	293.5	0.156	0.152
bcc Ca	–1357.5245	2.6	250.25		0.202	
fcc Sc	–1524.9902		150.26		0.541	
bcc Sc	–1524.9863	3.9	153.08		0.597	
fcc Ti	–1703.9688		108.04		1.260	
bcc Ti	–1703.9670	1.8	107.54		1.257	
fcc V	–1894.7593		87.92		2.081	
bcc V	–1894.7870	–27.7	84.63	93.7	2.230	1.619
fcc Cr	–2097.6747		75.83		2.651	
bcc Cr	–2097.7043	–29.6	74.06	81.0	3.056	1.903
fcc Mn	–2313.0172		68.87		3.351	
bcc Mn	–2313.0088	8.4	69.16		3.219	
fcc Fe	–2541.0881		65.55		3.387	
bcc Fe	–2541.0596	28.5	67.13	79.5	3.114	1.683
fcc Co	–2782.2037		65.73		2.487	
bcc Co	–2782.1804	23.3	65.93		3.539	
fcc Ni	–3036.6908		68.24	73.9	2.736	1.863
bcc Ni	–3036.6830	7.8	68.77		2.340	
fcc Cu	–3304.8630		74.29	79.7	1.424	1.309
bcc Cu	–3304.8574	5.6	76.07		3.121	
fcc Zn	–3586.7807		99.90		0.919	
bcc Zn	–3586.7716	9.1	94.33		0.789	

TABLE II. Bulk moduli ( $B_0$ ), equilibrium total energy ( $E_{\text{tot}}$ ), volume per atom ( $V_0$ ), and the total energy difference ( $\Delta E$ ) between bcc and fcc for 4d metals.

System	$E_{\text{tot}}$ (Ry)	$\Delta E$ (mRy)	$V_0$ (a.u. <sup>3</sup> )		$B_0$ (Mbar)	
			theor.	expt.	theor.	expt.
fcc Sr	-6352.1717		317.72	380.2	0.158	0.116
bcc Sr	-6352.1697	2.0	320.19		0.126	
fcc Y	-6763.6492		197.54		0.526	
bcc Y	-6763.6428	6.4	201.95		0.476	
fcc Zr	-7190.3942		146.47		1.047	
bcc Zr	-7190.3931	1.1	144.04		1.013	
fcc Nb	-7632.6227		120.81		1.798	
bcc Nb	-7632.6503	-27.6	116.94	121.4	1.948	1.702
fcc Mo	-8090.5781		104.42		2.564	
bcc Mo	-8090.6084	-30.3	102.89	105.2	2.881	2.725
fcc Tc	-8564.4862		94.50		2.996	
bcc Tc	-8564.4698	16.4	95.40		3.188	
fcc Ru	-9054.5830		90.18		3.548	
bcc Ru	-9054.5384	44.6	92.70		3.290	
fcc Rh	-9561.1185		90.85	92.9	3.116	2.705
bcc Rh	-9561.0855	33.0	93.41		2.785	
fcc Pd	-10084.3720		97.21	99.5	2.011	1.808
bcc Pd	-10084.3624	9.6	98.00		1.936	
fcc Ag	-10624.6357		110.85	115.1	1.131	1.007
bcc Ag	-10624.6261	9.6	112.03		1.268	
fcc Cd	-11181.7601		138.75		0.568	
bcc Cd	-11181.7526	7.5	141.36		0.562	

TABLE III. Bulk moduli ( $B_0$ ), equilibrium total energy ( $E_{\text{tot}}$ ), volume per atom ( $V_0$ ), and the total energy difference ( $\Delta E$ ) between bcc and fcc for 5d metals.

System	$E_{\text{tot}}$ (Ry)	$\Delta E$ (mRy)	$V_0$ (a.u. <sup>3</sup> )		$B_0$ (Mbar)	
			theor.	expt.	theor.	expt.
fcc Ba	-16265.8802		376.6		0.071	
bcc Ba	-16265.8818	-1.6	373.5	426.7	0.111	0.103
fcc La	-16982.1384		233.4		0.312	
bcc La	-16982.1332	5.2	240.4		0.307	
fcc Hf	-30177.1439		143.9		1.434	
bcc Hf	-30177.1435	0.4	143.3		1.247	
fcc Ta	-31233.3125		123.2		2.482	
bcc Ta	-31233.3382	-25.7	120.6	121.0	2.008	2.001
fcc W	-32312.9492		109.9		2.794	
bcc W	-32312.9878	-38.6	107.1	107.0	3.256	3.232
fcc Re	-33416.3614		100.1		3.533	
bcc Re	-33416.3427	18.7	100.5		3.743	
fcc Os	-34543.8631		94.7		4.419	
bcc Os	-34543.8039	59.2	98.2		3.783	
fcc Ir	-35695.7968		96.9	95.5	3.763	3.550
bcc Ir	-35695.7460	50.8	99.3		3.481	
fcc Pt	-36872.5535		102.6	101.9	3.335	2.783
bcc Pt	-36872.5385	17.7	103.9		2.721	
fcc Au	-38074.5208		113.7	114.5	1.689	1.732
bcc Au	-38074.5122	8.6	116.4		1.763	
fcc Hg	-39301.8945		149.3		0.805	
bcc Hg	-39301.8903	4.2	159.1		0.374	
fcc Tl	-40554.9373		184.4		0.766	
bcc Tl	-40554.9311	6.2	189.4		0.339	
fcc Pb	-41833.9446		219.0	204.7	0.503	0.430
bcc Pb	-41833.9420	2.6	210.6		0.477	

band increases the strength of the  $d$  electron binding, which reaches its maximum at the middle of the  $d$  series. For the stable structures, a comparison with the results of Moruzzi, Janak, and Williams<sup>7</sup> shows that the equilibrium volume and the bulk modulus are in good agreement. Small differences exist, however, which bring the calculations of Moruzzi, Janak, and Williams<sup>7</sup> to a slightly better agreement with experiment. The latter calculations were done also in the muffin-tin approximation by the Korringa-Kohn-Rostoker (KKR) method, but included no relativistic effects. Since the APW and KKR methods are considered equivalent and since we have checked the differences in  $k$ -point samplings between Moruzzi, Janak, and Williams<sup>7</sup> and our calculations, it is clear that the main source of discrepancies is the fact that our calculations include relativistic effects. The worsening of the agreement with experiment when relativistic corrections are included is an unexpected result that has also been found in the calculations of Elsässer *et al.*,<sup>19</sup> who attribute it to a cancellation of errors.

The structural energy difference  $\Delta E = E_{\text{tot}}(\text{fcc}) - E_{\text{tot}}(\text{bcc})$  also shown in Tables I–III has, with the exception of Fe, the correct sign predicting the stable structure between fcc and bcc, in agreement with experiment. We are not going to deal with the hcp structure in this paper. Fe was treated here with a paramagnetic calculation, but even the spin-polarized calculation does not produce the correct ground-state energy in the LDA.<sup>20</sup> Our equilibrium volumes and bulk moduli for bcc Sc, Ti, Mn, Co, and Ni are again in accord with the values found by Moruzzi and Marcus.<sup>16</sup>

The most complete study to date of the stability of the crystal structures across the periodic table was given by Skriver<sup>5</sup> using the LMTO method. Skriver based his approach on the findings of Pettifor and Andersen's force theorem, which lead to a cancellation of the double-counting term in the total energy and eliminates the core levels to a second-order approximation in the charge density. He also argues that the electrostatic term is in the range of 0.05–0.5 mRy and may be neglected. Therefore  $\Delta E$  involves only the sums of the valence one-electron energies. Using this methodology, Skriver calculated  $\Delta E$  from the expression

$$\Delta E = \int^{E_F} E N_{\text{bcc}}(E) dE - \int^{E_F} E N_{\text{fcc}}(E) dE$$

and correctly predicted the crystal structure of all transition metals except Au. However, Skriver's results, as well as those of Pettifor, are a factor of 3–5 larger than the enthalpy differences obtained by Miedema and Niessen<sup>21</sup> analyzing experimental phase diagrams.

In this work we have not employed any of the cancellation arguments of Pettifor and Skriver. We have subtracted total energies of the fcc and bcc structures retaining all terms in the total-energy expression. In all cases including Au our results give the correct crystal structure. Since Skriver did not tabulate his results for  $\Delta E$ , we can only compare with a graph shown in his paper for the  $4d$  elements. For those elements like Nb, Mo, Ru, and Rh that have large  $\Delta E$  the agreement is very good. For elements with small  $\Delta E$  the comparison is not easy, but it

is clear that we agree on the sign of  $\Delta E$ . A comparison with Miedema and Niessen's analysis shows that the theory still overestimates the "experimental" results. In the  $5d$  series our results shown in Table III are also in good agreement with those of Skriver, especially for those elements in the middle of the series that have large  $\Delta E$  values. It should be noted, however, that we get the correct structure, with  $\Delta E = 8.6$  mRy even for Au, where Skriver's calculation failed. Our results for the  $5d$  elements are also in agreement with the work of Davenport, Watson, and Weinert,<sup>6</sup> who used the augmented-Slater-type-orbital method. Again, a detailed comparison of the  $\Delta E$  values is not available with the results of Davenport, Watson, and Weinert, but from their graph of  $\Delta E$  versus element one observes the same trends.

In the process of the present study we have discovered the following prescription to obtain essentially the same results for  $\Delta E$ . This is done by performing only the fcc calculations self-consistently. Then for the bcc calculations we use the self-consistent fcc charge density to construct a bcc potential for a lattice constant corresponding to equal fcc and bcc volumes. This potential is used to perform only one iteration with the APW program. The resulting total energy agrees with that of the fully self-consistent bcc calculation to an accuracy of approximately 0.5 mRy. We applied this procedure to Al, V, and Co with equal success. Our prescription appears to be similar to Skriver's approach and is in the same spirit as the Harris approximation.<sup>22</sup>

The relative stability of the elements described by the quantity  $\Delta E$  is of great importance in the construction of phase diagrams. Miedema and Niessen<sup>21</sup> as well as Kaufman and Bernstein<sup>23</sup> have utilized experimental data to obtain estimates of  $\Delta E$ . These results are smaller than the theoretical  $\Delta E$  by factors as large as 3. The source of this discrepancy is not understood at present. On the theoretical side the muffin-tin approximation employed in this work cannot account for the error. Calculations that have removed this approximation, such as that of Jansen and Freeman<sup>24</sup> for W and of Singh and Papaconstantopoulos<sup>11</sup> for Zn, show very small effect on  $\Delta E$ .

#### IV. TRENDS IN THE BAND STRUCTURE

In Tables IV–VI we list characteristic energies for the  $\Gamma_1$  state, the bottom and top of the  $d$  bands, and the Fermi energy  $E_F$ . In our notation  $E_{db}$  denotes the bottom of the  $d$  bands and corresponds to the state  $X_1$  or  $L_1$  for the fcc metals and the state  $N_1$  or  $H_{12}$  for the bcc metals.  $E_{dt}$  denotes the top of the  $d$  bands and corresponds to the states  $W'_1$  and  $N_3$  for fcc and bcc, respectively. It can be seen from Tables IV–VI that the  $d$ -band width  $\Delta E_d$  increases across each row for both fcc and bcc structures, up to a maximum in the (V,Nb,Ta) column and then decreases slowly as the  $d$  band fills up. Looking at a given column in the Periodic Table we note that  $\Delta E_d$  increases from the  $3d$  to the  $5d$  metals. Also from Tables IV–VI we can form the difference  $E_F - E(\Gamma_1)$ , which is a measure of the occupied valence bands. This quantity increases across the different rows and reaches a maximum in the (Co,Rh,Ir) column. It is worth noting that the oc-

TABLE IV. Theoretical energies for the  $\Gamma_1$  state, the bottom ( $E_{db}$ ), the top ( $E_{dt}$ ), and the width ( $\Delta E_d$ ) of the  $d$  band, and the Fermi energy ( $E_F$ ) for the 3*d* metals.

System	$\Gamma_1$ (Ry)	$E_{db}$ (Ry)	$E_{dt}$ (Ry)	$\Delta E_d$ (Ry)	$E_F$ (Ry)
fcc Ca	0.085	0.244	0.650	0.406	0.313
bcc Ca	0.040	0.285	0.730	0.445	0.382
fcc Sc	0.094	0.347	0.812	0.465	0.488
bcc Sc	0.128	0.383	0.882	0.499	0.554
fcc Ti	0.172	0.404	0.932	0.528	0.628
bcc Ti	0.207	0.454	0.996	0.542	0.678
fcc V	0.232	0.451	1.207	0.576	0.751
bcc V	0.275	0.509	1.101	0.592	0.815
fcc Cr	0.209	0.440	0.989	0.549	0.770
bcc Cr	0.261	0.505	1.076	0.571	0.878
fcc Mn	0.196	0.443	0.983	0.540	0.828
bcc Mn	0.236	0.503	1.076	0.549	0.903
fcc Fe	0.174	0.445	0.973	0.528	0.867
bcc Fe	0.172	0.472	0.978	0.506	0.868
fcc Co	0.073	0.382	0.820	0.438	0.773
bcc Co	0.116	0.439	0.900	0.461	0.825
fcc Ni	0.006	0.337	0.712	0.375	0.695
bcc Ni	0.010	0.347	0.715	0.368	0.710
fcc Cu	-0.071	0.268	0.568	0.300	0.664
bcc Cu	-0.057	0.269	0.566	0.297	0.670
fcc Zn	-0.214	-0.040	0.125	0.125	0.636
bcc Zn	-0.176	0.006	0.151	0.145	0.684

cupied bandwidth is the largest for the 5*d* series where the state  $\Gamma_1$  is pulled down more than in the 3*d* and 4*d* rows due to a strong relativistic effect on the  $s$ -like  $\Gamma_1$  state. In Tables VII and VIII we show the position and width of the occupied 3*p* and 4*p* bands for the fcc structure. In the bcc structure these widths are of similar size. These bands are deep in energy and very narrow. As we move across the rows we note that the  $p$  bands lie deeper

in energy, starting, for example, with 1.65 Ry below  $E_F$  for Ca and going to 6.0 Ry below  $E_F$  for Zn. On the other hand, the  $p$ -band width increases from Ca (Sr) to Cr(Mo) near the center of the series and then decreases rapidly toward Zn (Cd). This behavior seems to correlate with the variation of the lattice constant. For the 5*d* elements, we did not treat the 5*p* levels as bands but as core levels. This was done in order to handle these levels fully

TABLE V. Theoretical energies for the  $\Gamma_1$  state, the bottom ( $E_{db}$ ), the top ( $E_{dt}$ ), and the width ( $\Delta E_d$ ) of the  $d$  band, and the Fermi energy ( $E_F$ ) for the 4*d* metals.

System	$\Gamma_1$ (Ry)	$E_{db}$ (Ry)	$E_{dt}$ (Ry)	$\Delta E_d$ (Ry)	$E_F$ (Ry)
fcc Sr	0.012	0.210	0.704	0.494	0.295
bcc Sr	0.033	0.235	0.767	0.532	0.330
fcc Y	0.144	0.326	1.010	0.684	0.506
bcc Y	0.092	0.296	0.899	0.603	0.469
fcc Zr	0.187	0.340	1.072	0.732	0.608
bcc Zr	0.188	0.369	1.083	0.714	0.625
fcc Nb	0.267	0.371	1.185	0.814	0.740
bcc Nb	0.285	0.408	1.242	0.834	0.795
fcc Mo	0.191	0.305	1.015	0.710	0.684
bcc Mo	0.264	0.374	1.167	0.793	0.835
fcc Tc	0.194	0.293	1.005	0.712	0.751
bcc Tc	0.214	0.330	1.054	0.724	0.808
fcc Ru	0.191	0.276	0.973	0.697	0.795
bcc Ru	0.185	0.299	0.974	0.675	0.789
fcc Rh	0.083	0.198	0.759	0.561	0.681
bcc Rh	0.103	0.234	0.798	0.564	0.679
fcc Pd	0.012	0.135	0.589	0.454	0.565
bcc Pd	0.028	0.162	0.610	0.447	0.561
fcc Ag	-0.088	0.010	0.306	0.296	0.490
bcc Ag	-0.060	0.048	0.370	0.322	0.550
fcc Cd	-0.202	-0.245	-0.113	0.132	0.502
bcc Cd	-0.193	-0.255	-0.132	0.123	0.474

TABLE VI. Theoretical energies for the  $\Gamma_1$  state, the bottom ( $E_{db}$ ), the top ( $E_{dt}$ ), and the width ( $\Delta E_d$ ) of the  $d$  band, and the Fermi energy ( $E_F$ ) for the  $5d$  metals.

System	$\Gamma_1$ (Ry)	$E_{db}$ (Ry)	$E_{dt}$ (Ry)	$\Delta E_d$ (Ry)	$E_F$ (Ry)
fcc Ba	0.074	0.202	0.686	0.484	0.282
bcc Ba	0.089	0.223	0.740	0.517	0.296
fcc La	0.210	0.273	0.961	0.688	0.448
bcc La	0.208	0.291	0.983	0.692	0.449
fcc Hf	0.063	0.331	1.143	0.813	0.659
bcc Hf	0.081	0.351	1.202	0.851	0.639
fcc Ta	0.081	0.330	1.193	0.863	0.690
bcc Ta	0.118	0.376	1.288	0.913	0.749
fcc W	0.068	0.307	1.163	0.857	0.735
bcc W	0.108	0.355	1.256	0.901	0.843
fcc Re	0.059	0.281	1.136	0.854	0.800
bcc Re	0.088	0.323	1.208	0.881	0.889
fcc Os	0.020	0.239	1.043	0.804	0.813
bcc Os	0.043	0.277	1.089	0.812	0.854
fcc Ir	-0.050	0.1712	0.865	0.693	0.754
bcc Ir	-0.030	0.202	0.904	0.701	0.742
fcc Pt	-0.115	0.106	0.687	0.581	0.646
bcc Pt	-0.088	0.134	0.734	0.600	0.643
fcc Au	-0.196	0.002	0.435	0.423	0.533
bcc Au	-0.175	0.025	0.460	0.435	0.550
fcc Hg	-0.302	-0.199	0.002	0.202	0.416
bcc Hg	-0.294	-0.208	-0.030	0.179	0.376
fcc Tl	-0.395	-0.504	-0.423	0.081	0.345
bcc Tl	-0.358	-0.493	-0.419	0.074	0.440

TABLE VII. The bottom ( $E_b$ ), the top ( $E_t$ ), and the bandwidth ( $dE$ ) of the  $3p$  band for the fcc  $3d$  metals in the equilibrium lattice constant ( $a_0$ ).

Element	$a_0$ (a.u.)	$E_b$ (Ry)	$E_t$ (Ry)	$dE$ (Ry)
Ca	10.02	-1.338	-1.322	0.016
Sc	8.42	-1.544	-1.501	0.043
Ti	7.57	-1.782	-1.717	0.065
V	7.04	-2.044	-1.967	0.077
Cr	6.73	-2.362	-2.287	0.075
Mn	6.51	-2.698	-2.630	0.068
Fe	6.39	-3.069	-3.014	0.055
Co	6.40	-3.489	-3.451	0.037
Ni	6.49	-3.950	-3.928	0.022
Cu	6.68	-4.471	-4.461	0.010
Zn	7.28	-5.316	-5.314	0.002

TABLE VIII. The bottom ( $E_b$ ), the top ( $E_t$ ), and the bandwidth ( $dE$ ) of the  $4p$  band for the fcc  $4d$  metals in the equilibrium lattice constant ( $a_0$ ).

Element	$a_0$ (a.u.)	$E_b$ (Ry)	$E_t$ (Ry)	$dE$ (Ry)
Sr	10.860	-1.049	-1.024	0.025
Y	9.235	-1.210	-1.150	0.050
Zr	8.385	-1.409	-1.322	0.087
Nb	7.825	-1.620	-1.515	0.105
Mo	7.480	-1.870	-1.764	0.106
Tc	7.235	-2.136	-2.035	0.101
Ru	7.110	-2.424	-2.340	0.084
Rh	7.150	-2.755	-2.698	0.057
Pd	7.305	-3.115	-3.082	0.033
Ag	7.615	-3.559	-3.545	0.014
Cd	8.240	-4.222	-4.219	0.003

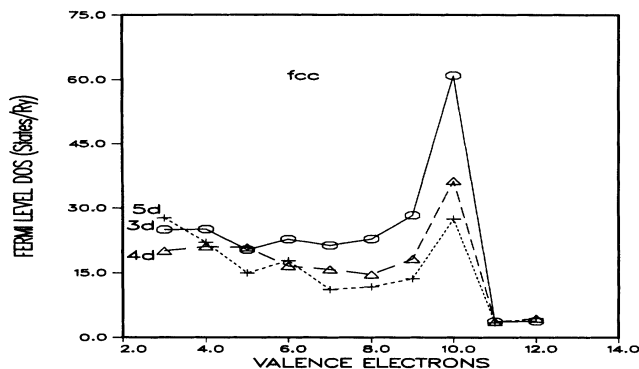


FIG. 1. Density of states at the Fermi level as a function of valence electrons for the fcc metals.

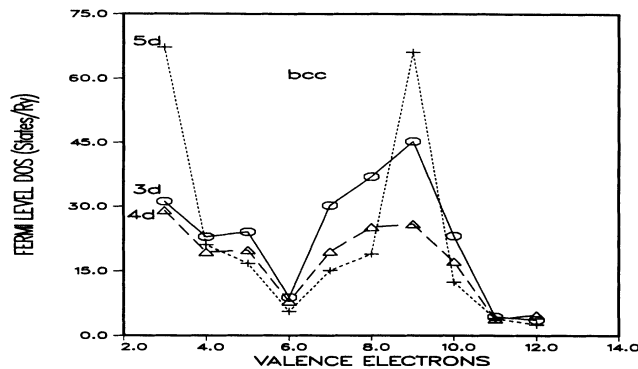


FIG. 2. Density of states at the Fermi level as a function of valence electrons for the bcc metals.

relativistically including the spin-orbit interaction.

In Figs. 1 and 2 we present the density of states,  $N(E_F)$  at  $E_F$ , as a function of valence electrons  $Z$ . In the fcc structure (Fig. 1)  $N(E_F)$  is fairly constant across each row but abruptly increases to a maximum for  $Z=10$ , which corresponds to the (Ni,Pd,Pt) column. It is significant to note that Ni and Pd have the highest  $N(E_F)$  from all the fcc metals, consistent with the occurrence of magnetism in Ni and often speculated magnetic instability in Pd. In the bcc structure (Fig. 2) we observe a wider variation of  $N(E_F)$ , with a pronounced minimum at  $Z=6$  (Cr,Mo,W) and a rapid increase for larger  $Z$  reaching a maximum at  $Z=9$  (Co,Rh,Ir). Iridium, which appears to have a very large  $N(E_F)$  in the bcc structure, is stable in the fcc structure, as our total-energy calculations confirm. However, it may be that Ir is a good candidate for synthesis in the bcc structure and for either superconductivity or magnetism. Finally, we point out the also very large  $N(E_F)$  of bcc La, which is consistent with the findings of Lu, Singh, and Krakauer.<sup>25</sup>

## V. SUMMARY

We presented a systematic study of the crystal structure stability between fcc and bcc for all the 3d, 4d, and 5d metals including the alkaline-earth elements. Our results predict the correct crystal structure for all elements except for Fe in agreement with previous works. Equilibrium lattice parameters and bulk moduli have the usual, in the LDA, small discrepancies from experiment with the 5d series giving the best agreement. We also presented a compendium of characteristic bandwidths and Fermi level values of density of states across the Periodic Table.

## ACKNOWLEDGMENTS

We wish to thank A. C. Switendick, M. J. Mehl, and D. Singh for many discussions and suggestions. This work was supported by PENED program 100/1989 from the Greek Secretariat of Science and Technology, by a NATO travel grant, and by the U. S. Office of Naval Research.

<sup>1</sup>D. G. Pettifor, *J. Phys. C* **3**, 367 (1970).

<sup>2</sup>A. R. MacKintosh and O. K. Andersen, in *Electrons at the Fermi Surface*, edited by H. Springford (Cambridge University Press, Cambridge, 1980).

<sup>3</sup>O. K. Andersen, H. L. Skriver, H. Nohl, and B. Johansson, *Pure Appl. Chem.* **52**, 93 (1979).

<sup>4</sup>V. Heine, in *Solid State Physics*, edited by H. Ehrenreich, F. Seitz, and D. Turnbull (Academic, New York, 1980), Vol. 35, p. 119.

<sup>5</sup>H. L. Skriver, *Phys. Rev. B* **31**, 1909 (1984).

<sup>6</sup>J. W. Davenport, R. E. Watson, and M. Weinert, *Phys. Rev. B* **32**, 4883 (1985).

<sup>7</sup>V. L. Moruzzi, J. F. Janak, and A. R. Williams, *Calculated Electronic Properties of Metals* (Pergamon, New York, 1978).

<sup>8</sup>J. F. Janak, *Phys. Rev. B* **9**, 3985 (1974).

<sup>9</sup>L. F. Mattheiss, J. H. Wood, and A. C. Switendick, *Methods Comput. Phys.* **8**, 63 (1968).

<sup>10</sup>M. Sigalas, N. C. Bacalis, D. A. Papaconstantopoulos, M. J. Mehl, and A. C. Switendick, *Phys. Rev. B* **42**, 11 637 (1990).

<sup>11</sup>D. Singh and D. A. Papaconstantopoulos, *Phys. Rev. B* **42**, 8885 (1990).

<sup>12</sup>D. D. Koelling and B. N. Harmon, *J. Phys. C* **10**, 3107 (1977).

<sup>13</sup>L. Hedin and B. I. Lundqvist, *J. Phys. C* **4**, 2064 (1971).

<sup>14</sup>F. Birch, *J. Geophys. Res.* **83**, 1257 (1978).

<sup>15</sup>K. A. Gschneidner, Jr., *Solid State Phys.* **16**, 276, (1964).

<sup>16</sup>V. L. Moruzzi and P. M. Marcus, *Phys. Rev. B* **38**, 1613 (1988).

<sup>17</sup>V. L. Moruzzi, P. M. Marcus, K. Schwarz, and P. Mohn, *Phys. Rev. B* **34**, 1784 (1986).

<sup>18</sup>R. A. Stager and H. G. Drickamer, *Phys. Rev.* **131**, 2524 (1963).

<sup>19</sup>C. Elsässer, N. Takeuchi, K. M. Ho, C. T. Chan, P. Braun, and M. Fahnle, *J. Phys. Condens. Matter* **2**, 4371 (1990).

<sup>20</sup>C. S. Wang, B. M. Klein, and H. Krakauer, *Phys. Rev. Lett.* **54**, 1852 (1985).

<sup>21</sup>A. R. Miedema and A. K. Niessen, *Comput. Coupling Phase Diagrams Thermoch.* **7**, 27 (1983).

<sup>22</sup>J. Harris, *Phys. Rev. B* **31**, 1770 (1985).

<sup>23</sup>L. Kauffman and H. Bernstein, *Computer Calculation of Phase Diagrams* (Academic, New York, 1970).

<sup>24</sup>H. J. F. Jansen and A. J. Freeman, *Phys. Rev. B* **30**, 561 (1984).

<sup>25</sup>Z. W. Lu, D. J. Singh, and H. Krakauer, *Phys. Rev. B* **39**, 4921 (1989).